

# Coordination Modes of 2,5-Di(*tert*-butyl)pyrrolide – Crystal Structures of HPyr\*, Pyr\*H·thf, (thf)<sub>2</sub>LiPyr\*, and [(Me<sub>3</sub>Si)<sub>3</sub>C-Zn]<sub>2</sub>(μ-Cl)(μ-Pyr\*) (Pyr\* = 2,5-*t*Bu<sub>2</sub>NC<sub>4</sub>H<sub>2</sub>)

Matthias Westerhausen<sup>a\*</sup>, Michael Wieneke<sup>a</sup>, Heinrich Nöth<sup>a†</sup>, Thomas Seifert<sup>a†</sup>, Arno Pfitzner<sup>b,†</sup>, Wolfgang Schwarz<sup>c†</sup>, Oliver Schwarz<sup>c</sup>, and Johann Weidlein<sup>\*c</sup>

Institut für Anorganische Chemie der Ludwig-Maximilians-Universität München<sup>a</sup>,  
Meiserstraße 1, D-80333 München, Germany  
Fax: (internat.) + 49(0)89/5902-578  
E-mail: maw@anorg.chemie.uni-muenchen.de

Institut für Anorganische Chemie der Universität Siegen<sup>b</sup>,  
Adolf-Reichwein-Straße, D-57068 Siegen, Germany

Institut für Anorganische Chemie der Universität Stuttgart<sup>c</sup>,  
Pfaffenwaldring 55, D-70569 Stuttgart, Germany  
Fax: (internat.) +49(0)711/685-4241

Received March 30, 1998

**Keywords:** Hydrogen bonds / Indium / Lithium / Nitrogen heterocycles / Zinc

The lithiation of 2,5-di(*tert*-butyl)pyrrole (**1**) yields bis(tetrahydrofuran)lithium 2,5-di(*tert*-butyl)pyrrolide (**2**), which is monomeric in solution as well as in the solid state. Due to the coordination number of three for the lithium atom, short Li–O and Li–N bond lengths of 193 pm are observed. The metathesis reaction of **2** with tris(trimethylsilyl)methylzinc chloride (**3**) gives colorless bis[tris(trimethylsilyl)methylzinc] chloride 2,5-di(*tert*-butyl)pyrrolide (**4**). The pyrrolide ligand and the chlorine atom bridge the zinc atoms. One of the zinc atoms is bonded to the nitrogen atom of the

pyrrolide substituent, while the other bonds to the opposite C–C bond. At 215 pm, the Zn–N bond is very long compared to those in alkylzinc amides, whereas the Zn–C distances lie in the range of Zn–C bond lengths found between zinc and η<sup>5</sup>-bonded cyclopentadienide ligands. The molecular structures of **1** and of the low-melting THF adduct **1**·thf show a similar 2,5-di(*tert*-butyl)pyrrole molecule, but in the latter case a weak N–H···O bond is observed (N–H 97 pm, O···H 199 pm).

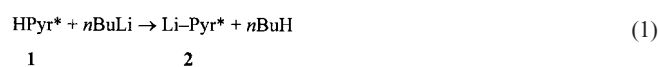
The pyrrolide substituent [NC<sub>4</sub>H<sub>4</sub>]<sup>−</sup> is isoelectronic with the cyclopentadienide anion, and since it possesses 6π electrons can be regarded as a Hückel aromatic system. In contrast to this (formal) analogy of these ligands, the substitution of a cyclopentadienide ligand of the well-known ferrocene by a pyrrolide substituent to yield an azaferrocene was first reported in 1963.<sup>[1]</sup> The significantly lower tendency of the NC<sub>4</sub>H<sub>4</sub><sup>−</sup> anion to coordinate as a π ligand and the enhanced tendency to form M–N σ bonds is a consequence of the high electronegativity of the heteroatom. On the other hand, the bonding properties depend on the substitution pattern on the pyrrolide ring. In 2,2',5,5'-tetramethyl-1,1'-diazaplumbocene, η<sup>1</sup> bonding to the 2,5-dimethylpyrrolide is observed,<sup>[2]</sup> whereas the corresponding 2,5-di-*tert*-butyl-substituted pyrrolide crystallizes with an η<sup>5</sup>-bonded ring.<sup>[3]</sup> In contrast to these findings, the group-13 metals (boron group, triels) form derivatives of the type Me<sub>2</sub>M<sup>III</sup>NC<sub>4</sub>H<sub>4-x</sub>R<sub>x</sub> with σ(M–N) bonds (η<sup>1</sup> coordination), although in the solid state the M<sup>III</sup> metal centers are also bonded to the π-system of a pyrrolide ligand of a neighboring molecule, thus forming π associates.<sup>[4]</sup>

Here, we describe three different coordination modes of the 2,5-di(*tert*-butyl)pyrrolide anion Pyr\*<sup>−</sup>. This ligand forms Li–N σ bonds, but the reaction of LiPyr\* with InCl<sup>[5]</sup> yields the indium(I) derivative with a η<sup>5</sup>-bonded Pyr\* anion. The unusual bridging mode is found to be adopted in bis[tris(trimethylsilyl)methylzinc] chloride 2,5-di(*tert*-butyl)pyrrolide. For the sake of comparison, the molecular structures of 2,5-di(*tert*-butyl)pyrrole and of its tetrahydrofuran complex are also included.

## Results

### Preparation

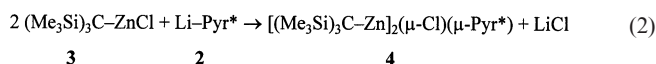
The starting material 2,5-di(*tert*-butyl)pyrrole<sup>[6]</sup> (H–Pyr\*, **1**), which crystallizes from a concentrated tetrahydrofuran solution as a THF solvate (**1**·thf), has been well known for more than 30 years. With *n*-butyllithium, **1** is lithiated according to eq. 1 to give quantitatively bis(tetrahydrofuran-*O*)lithium 2,5-di(*tert*-butyl)pyrrolide (**2**).



Meanwhile, the reaction of lithium tris(trimethylsilyl)methanide with anhydrous ZnCl<sub>2</sub> yields [(thf)<sub>4</sub>Li][(Me<sub>3</sub>Si)<sub>3</sub>-

<sup>[†]</sup> X-ray structure analysis.

$\text{CZn}_2(\mu\text{-Cl})_3$ . In order to obtain a product free from lithium halide and THF, tris(trimethylsilyl)methylzinc chloride (**3**) was purified by sublimation. Reactions of **3** with alkyl- and phenyllithium compounds yield the heteroleptic compounds  $(\text{Me}_3\text{Si})_3\text{C-Zn-R}$ , which have in part been characterized by X-ray crystallography.<sup>[7]</sup> All these derivatives are monomeric and contain solely  $\sigma(\text{Zn-C})$  bonds. The metathesis reaction of **3** with  $(\text{thf})_2\text{LiPyr}^*$  (**2**) (eq. 2) yields bis-[tris(trimethylsilyl)methylzinc] chloride 2,5-di(*tert*-butyl)pyrrolide (**4**) as a colorless and moisture-sensitive solid with a melting point of 74–75°C.



The stoichiometry of this metathesis reaction obeys a 2:1 ratio, irrespective of the molar ratio of the reactants. Stirring or refluxing of a 1:1 mixture of the starting materials does not lead to the formation of a halogen-free derivative, as is known for the metathesis reactions with lithium alkanides.<sup>[7]</sup> The cryoscopically determined molecular mass of **4** is consistent with the proposed structure shown in eq. 2. Dissociation into **3** and mononuclear, heteroleptic tris(trimethylsilyl)methylzinc 2,5-di(*tert*-butyl)pyrrolide does not occur under these conditions.

Indium(I) chloride reacts with lithiated 2,5-dimethyl-, 2,3,4,5-tetramethyl- as well as 2,5-di-*tert*-butylpyrrole in toluene, hexane, or tetrahydrofuran at low temperatures. However, the expected products of the methyl-substituted species are not isolable, since decomposition occurs even at temperatures of –90°C and –30°C, respectively, and precipitation of indium metal is observed. In contrast to this instability, indium(I) 2,5-di(*tert*-butyl)pyrrolide  $\text{In}^{\text{I}}[\text{Pyr}^*]$  (**5**), which forms in tetrahydrofuran at low temperatures according to eq. 3, can be isolated and purified by distillation or sublimation in vacuo. During the melting of **5** at 77–78°C, the compound turns grey. The volatility of  $\text{In}^{\text{I}}[\text{Pyr}^*]$  (**5**) is comparable to that of hexameric (pentamethylcyclopentadienyl)indium [pentamethylindocene(I)].<sup>[8]</sup> The sensitivities of these compounds towards oxygen are also similar, since  $\text{In}^{\text{I}}[\text{Pyr}^*]$  (**5**) decomposes immediately with precipitation of metallic indium.



### Molecular Structures

For comparison purposes, the molecular structure of  $\text{HPyr}^*$  (**1**) is briefly described. Suitable single crystals form during the sublimation of **1** at 35°C in vacuo. The molecular structure is shown in Figure 1. The asymmetric unit contains three crystallographically independent molecules, which are distinguished by the first digit  $n = 1, 2$  and  $3$  following the element symbol. The delocalization within the five-membered ring is disturbed, as is evident from the bond lengths of 137 pm for  $\text{C}(n1)\text{-C}(n2)$  and  $\text{C}(n3)\text{-C}(n4)$ , and the value of 142 pm for  $\text{C}(n2)\text{-C}(n3)$ . The bond

lengths  $\text{N}(n)\text{-H}(n)$  fall in the narrow range from 83 to 91 pm.

The molecular structure of the tetrahydrofuran complex **1**·thf is depicted in Figure 2. This adduct shows a crystallographically imposed  $C_{2v}$  symmetry. The bond lengths in the pyrrole ring are not affected by coordination of a tetrahydrofuran molecule to the  $\text{N1-H1}$  group. Even the  $\text{N1-H1}$  distance of 97 pm differs only by 3 times the esd. On the other hand, the  $\text{O2}\cdots\text{H1}$  contact of 199 pm is quite long (cf. the  $\text{O-H}$  distances in ice, which vary between 99 and 176 pm). This weak interaction explains the low melting point of **1**·thf (below 0°C).

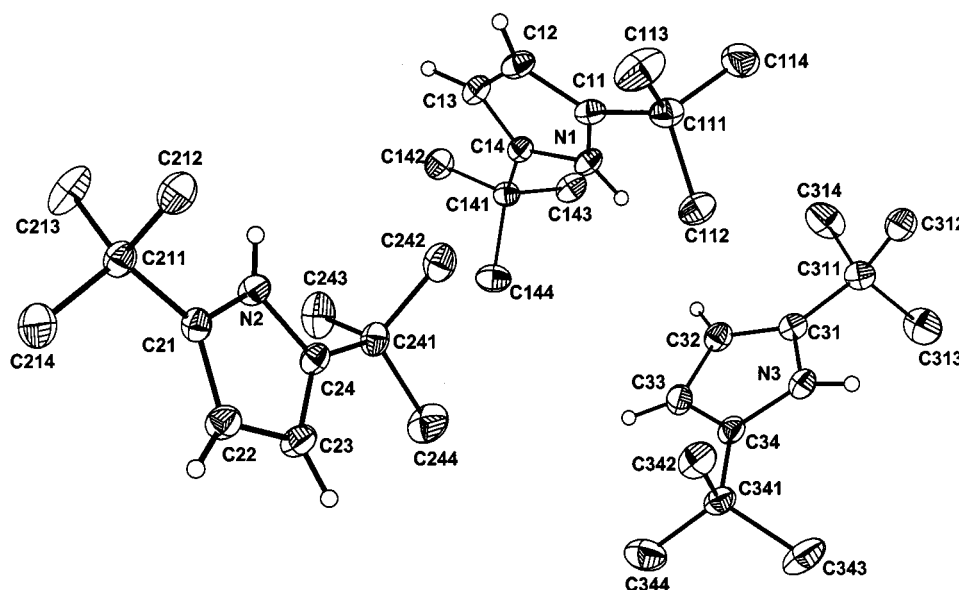
The molecular structure of lithium 2,5-di(*tert*-butyl)pyrrolide (**2**) is shown in Figure 3. To date, only one related molecule has been described in the literature, namely an *N*-lithiocarbazole dimer. Compound **2** crystallizes as a monomer due to the steric shielding of the lithium atom by the *tert*-butyl groups. The lithium atom is in a trigonal-planar coordination sphere, with a short  $\text{Li-N}$  bond length of 193 pm. The low coordination number of the alkali metal is also the reason for the short  $\text{Li-O}$  distances of 193 pm. In comparison to **1**, the endocyclic  $\text{C-C}$  bond lengths in the pyrrolide ligand of **2** are 138 and 140 pm for  $\text{C1-C2}$  and  $\text{C2-C2}'$ , respectively, and are therefore very similar.

The molecular structure of **4** is depicted in Figure 4. The molecule contains a crystallographic mirror plane, although this symmetry element does not indicate the molecular symmetry, but rather leads to a two-site disorder of the 2,5-di(*tert*-butyl)pyrrolide ligand. However, only one orientation is shown in Figure 4. The atoms generated by the crystallographic mirror plane are marked with apostrophes. The two zinc atoms of the isomer shown in Figure 4 are in different environments;  $\text{Zn}$  has a coordination number of four, whereas  $\text{Zn}'$  is threefold coordinated by the atoms  $\text{C1}'$ ,  $\text{Cl}$  and  $\text{N2}$ .

The chlorine atom bridges the two zinc atoms with  $\text{Zn-Cl}$  bond lengths of 241 pm and a  $\text{Zn-Cl-Zn}'$  bond angle of 110.3°. Terminal  $\text{Zn-Cl}$  bond lengths, as for example in  $(\text{bpy})\text{ZnCl}_2$ <sup>[10]</sup> or  $(\text{tmeda})\text{Zn}(\text{Cl})\text{R}$ <sup>[11]</sup> are typically around 225 pm, and similar values are observed for various zinc(II) chloride modifications.<sup>[12]</sup> The  $\text{Zn-Cl}$  distances in dimeric  $(\text{Me}_2\text{PhSi})_3\text{C-Zn-Cl}$ <sup>[13]</sup> as well as in dimeric  $\text{F}_3\text{C-CCl}_2\text{-Zn}(\text{OEt}_2)\text{Cl}$ <sup>[14]</sup> are distinctly shorter (average 233 pm) than those in **4**. Moreover, the endocyclic  $\text{Zn-Cl-Zn}$  angle is approximately 18° smaller than the corresponding angle in **4**. This distortion of the  $(\text{RZn})_2\text{Cl}$  moiety is due to the 2,5-di-*tert*-butylpyrrolide ligand, which also bridges the two zinc atoms. The planes  $\text{Cl/Zn/Zn}'$  and  $\text{N2/C21/C22/C23/C24}$  are oriented almost perpendicular to one another, with an angle between their normals of 93.5°.

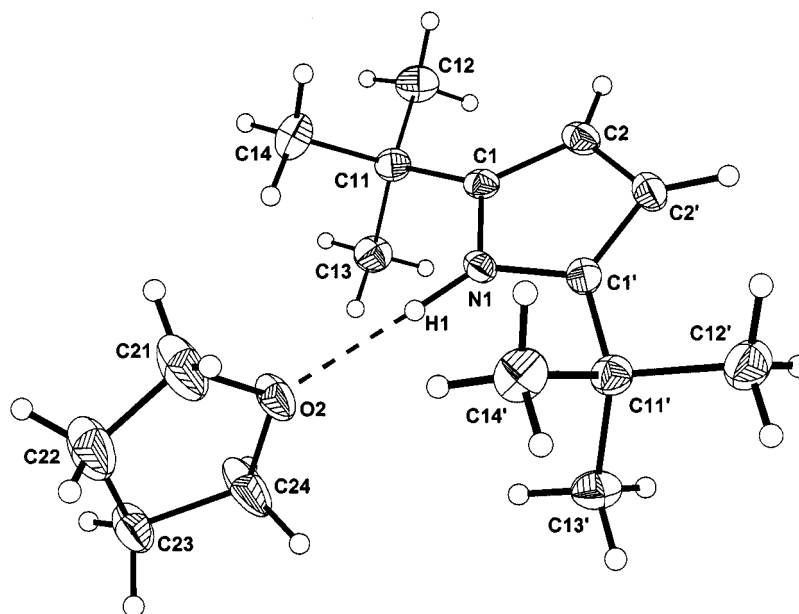
Sterically uncrowded cyclopentadienyl complexes of zinc tend to form polymers. Whereas methyl(cyclopentadienyl)zinc is monomeric in the gaseous phase, it polymerizes in the solid state to form a structure with bridging  $\text{C}_5\text{H}_5^-$  ligands and the metal atoms on opposite sides of the aromatic rings.<sup>[15]</sup> Analogous behavior is observed for bis-(cyclopentadienyl)zinc with a bridging and a terminal  $\eta^1$ -bonded ligand.<sup>[16]</sup> In the gas phase, monomeric decamethyl-

Figure 1. Molecular structure and numbering scheme of the asymmetric unit of HPyr\* (1); the ellipsoids represent a probability of 40%; the hydrogen atoms of the *tert*-butyl groups are omitted for clarity; those of the azacyclopentadiene unit are drawn with arbitrary radii<sup>[a]</sup>



<sup>[a]</sup> Selected bond lengths [pm]: N1–H1 85(2), N1–C11 137.2(3), N1–C14 138.3(3), C11–C12 136.4(3), C12–C13 141.8(4), C13–C14 137.1(3), N2–H2 83(3), N2–C21 137.5(3), N2–C24 137.8(3), C21–C22 136.5(3), C22–C23 142.4(3), C23–C24 136.3(3), N3–H3 91(3), N3–C31 139.0(3), N3–C34 136.3(3), C31–C32 135.7(4), C32–C33 141.8(4), C33–C34 137.0(3).

Figure 2. Molecular structure and numbering scheme of 1·thf; the ellipsoids represent a probability of 40% and the H atoms are drawn with arbitrary radii; the hydrogen bond is shown by a dotted line; symmetry-related atoms are marked with an apostrophe<sup>[a]</sup>

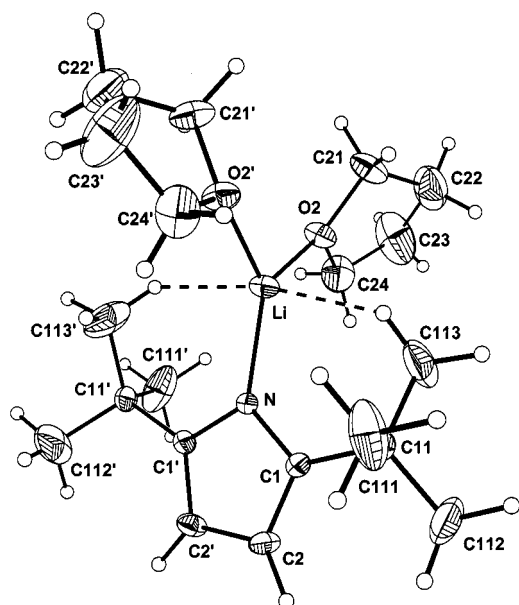


<sup>[a]</sup> Selected bond lengths [pm]: N1–H1 97(3), N1–C1 138.1(3), C1–C2 137.1(3), C2–C2' 141.1(5), O2–H1 199(3).

zincocene [bis(pentamethylcyclopentadienyl)zinc] has a structure of the type  $(\eta^1\text{-C}_5\text{Me}_5)(\eta^5\text{-C}_5\text{Me}_5)\text{Zn}$ .<sup>[17]</sup> The pyrrolide substituent in **3** is planar and shows a different coordination behavior. Both the zinc atoms coordinate at the same side of the ligand, but one zinc atom bonds via a  $\sigma(\text{Zn}-\text{N}2)$  bond whereas the other metal center shows an  $\eta^2$  coordination to the C22–C23 bond. The Zn–N2 bond

length of 215 pm is very long compared to the values in [tris(trimethylsilyl)methyl]zinc bis(trimethylsilyl)amide<sup>[11]</sup> (185 pm), in monomeric zinc bis(amides)<sup>[18]</sup> (characteristic value 182 pm), or even in bridging  $\mu$ -bonded bis(trimethylsilyl)amide substituents, where Zn–N distances of approximately 200 pm are found.<sup>[19]</sup> The Zn–N2 vector shows a deviation of 40.6° from an imaginary in-plane vector; the

Figure 3. Molecular structure and numbering scheme of  $(\text{thf})_2\text{Li-Pyr}^*$  (**2**); the ellipsoids represent a probability of 40%; the hydrogen atoms are drawn with arbitrary radii; symmetry-related atoms are marked with an apostrophe; agostic interactions between Li and the methyl groups are indicated with dotted lines<sup>[a]</sup>



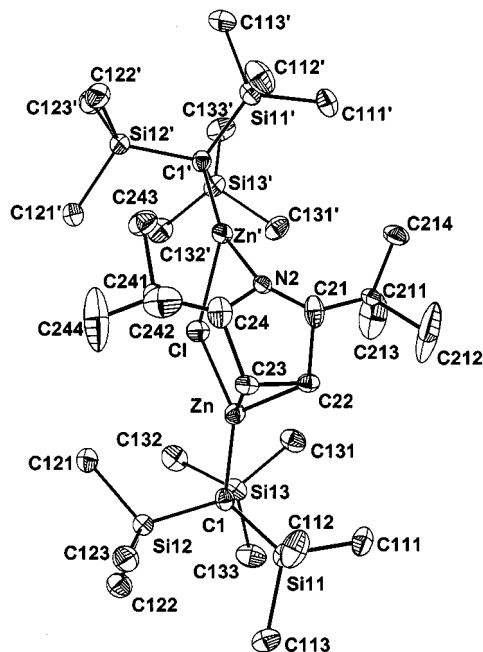
<sup>[a]</sup> Selected bond lengths [pm] and bond angles [°]: Li–N 193.2(7), Li–O2 192.6(4), N–C1 137.7(3), C1–C2 138.4(4), C2–C2' 140.4(5), N–Li–O2 127.4(2), O2–Li–O2' 105.3(3), Li–N–C1 127.0(1), C1–N–C1' 106.0(3).

N2-bonded zinc atom lies 143 pm above the calculated plane containing the atoms N2, C21, C22, C23, and C24.

The Zn–C22 and Zn–C23 distances of 219.0 and 219.4 pm fall within the broad range of values found for multi-hapto-bonded cyclopentadienide ligands. The chain-like zincocene<sup>[16]</sup> has Zn–C bond lengths between 204 and 241 pm, whereas in the zig-zag chain of methylzinc cyclopentadienide<sup>[15]</sup> Zn–C distances of 222 to 241 pm are observed. In both these molecules, the cyclopentadienide substituents bridge zinc atoms on opposite sides of the aromatic ring. Monomeric zincocenes such as decamethyl-, 1,1'-diphenyl- and 1,1'-bis(trimethylsilyl)zincocene<sup>[17]</sup> display one  $\eta^1$ -bonded (Zn–C 204–209 pm) and one  $\eta^5$ -coordinated cyclopentadienide ligand (217–230 pm). A similar bonding situation as in **4** is observed for dizinc tris(cyclopentadienide) bis(trimethylsilyl)amide (**A**)<sup>[19b]</sup> (Scheme 1), although the bridging ligand in this case is doubly  $\eta^1$ -coordinated; the third Zn–C distance of 250 pm is clearly too long to be considered as a bond.

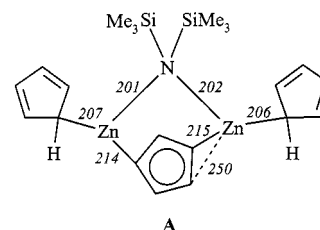
The bridging mode of the ligand  $\text{Pyr}^*$  is not very common, however, there are some other examples.<sup>[20]</sup> To the  $\sigma$ -bonded nitrogen heterocycles of tricarbonyl(diphenylaceto)manganese dipyrrolide a tricarbonylmanganese fragment is bonded side-on.<sup>[20a]</sup> Dicarbonylrhodium 2,5-dimethylpyrrolide dimerizes via an unsymmetric heterocycle bridge.<sup>[20b]</sup> The bridging mode of the pyrrolide anion in this molecule is quite similar to the geometry observed for **4** since the rhodium atoms do not lie above the center of the  $\text{NC}_5$  cycle. Solvent-free sodium tetramethylpyrrolide crystallizes as a

Figure 4. Molecular structure and numbering scheme of  $[(\text{Me}_3\text{Si})_3\text{CZn}]_2(\mu\text{-Cl})(\mu\text{-Pyr}^*)$  (**4**); the ellipsoids represent a probability of 40%; the disordering of the  $\text{Pyr}^*$  ligand is not shown (see text); all hydrogen atoms are omitted for clarity; symmetry-related atoms are marked with an apostrophe<sup>[a]</sup>



<sup>[a]</sup> Selected bond lengths [pm] and bond angles [°]: Zn–C1 201.3(4), Zn–Cl 241.0(1), Zn'–N2 215.1(6), N2–C21 126.1(7), N2–C24 127.5(8), Zn–C22 219.0(7), Zn–C23 219.4(7), C1–Si11 188.6(4), C1–Si12 188.8(4), C1–Si13 188.9(4); C1–Zn–Cl 120.2(1), C1'–Zn'–N2 155.1(2), Cl–Zn'–N2 84.7(2), Zn–Cl–Zn' 110.32(6).

Scheme 1. Selected bond lengths [pm] in tris(cyclopentadienyl)zinc  $\mu$ -bis(trimethylsilyl)amide (**A**)



polymer with a similar bridging pattern of the pyrrolide substituent.<sup>[20d]</sup> Kuhn et al.<sup>[20c]</sup> linked two octamethyl-1,1'-diazferrocene molecules via silver cations  $\sigma$ -bonded to the nitrogen atoms.

The Zn–C1 bond length in **4** exceeds the Zn–C bond lengths in [tris(trimethylsilyl)methyl]zinc derivatives  $(\text{Me}_3\text{Si})_3\text{C–Zn–R}$  with R as phenyl<sup>[7]</sup> (196 pm), bis(trimethylsilyl)methyl<sup>[7]</sup> (197 pm), and tris(trimethylsilyl)methyl<sup>[7][21]</sup> (198 pm); Zn–C bond lengths of sterically unstrained molecules are even shorter. All these findings are indicative of the steric strain within the molecule. The shielding of the  $\text{ClZn}_2$  moiety by the bulky substituents, which is illustrated in Figure 5, accounts for the fact that this molecule cannot react with a further equivalent of lithium 2,5-di(*tert*-butyl)pyrrolide (**2**).

Figure 5. Space-filling model of **4** viewed from the chlorine atom, showing the steric shielding of the Zn<sub>2</sub>Cl fragment

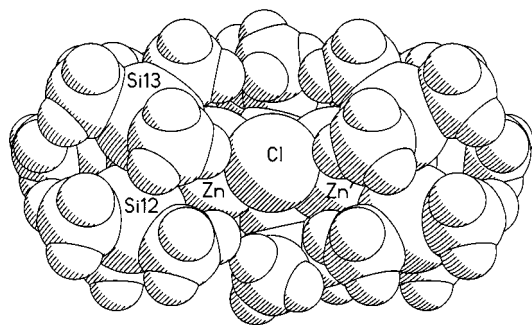
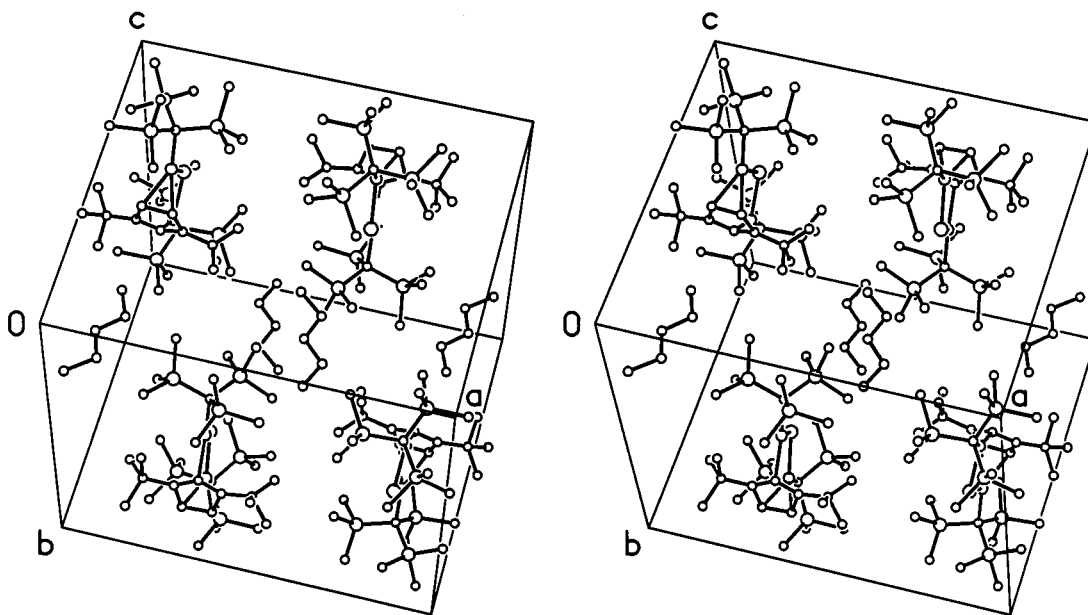


Figure 6 gives a stereoscopic view of the arrangement of **4**, together with the incorporated pentane. There are no significant intermolecular contacts; the pentane molecules lead to an additional separation of the molecules of **4**.

Figure 6. Stereoscopic representation of the molecular packing of **4** in the unit cell; the atoms are drawn with arbitrary radii and H atoms are omitted for clarity; the *n*-pentane molecules were refined with a fixed population factor of 0.67; the disordering of the 2,5-di(*tert*-butyl)pyrrolide ligand is not shown



### Spectroscopic Characterization

The NMR parameters of the 2,5-di-*tert*-butylpyrrolide ligands of **1–5** are compared in Table 1, along with data for Me<sub>2</sub>Ga–Pyr\*,<sup>[2]</sup> Me<sub>3</sub>Sn–Pyr\*,<sup>[2]</sup> Sn<sup>II</sup>[Pyr\*]<sub>2</sub>,<sup>[22]</sup> and Pb<sup>II</sup>–[Pyr\*]<sub>2</sub>.<sup>[3]</sup> The coordination mode of Pyr\* does not affect the NMR parameters of the *tert*-butyl groups. The influence of the hapticity of the pyrrolide ligand on the chemical shifts of the carbon atoms in the 2- and 5-positions is small, although η<sup>5</sup> coordination leads to a low-field shift of the <sup>13</sup>C resonances. The δ values of the carbon atoms in the 3- and 4-positions show no dependency on the coordination mode, except that in the case of the Sn<sup>IV</sup> derivative

Me<sub>3</sub>Sn–Pyr\*, the resonances of these nuclei are shifted to higher field by approximately 20 ppm.

Considering the molecular structure of the zinc derivative **2**, the magnetic equivalence of the tris(trimethylsilyl)methyl groups was not expected. However, the long distances between the zinc atoms and the pyrrolide substituent and the shape of the coordination gap allow a tilting motion, leading to a dynamic equilibrium through a Zn–N–Zn-bonded intermediate, in which the pyrrolide is rotated through approximately 90°. This situation is depicted in eq. 4.

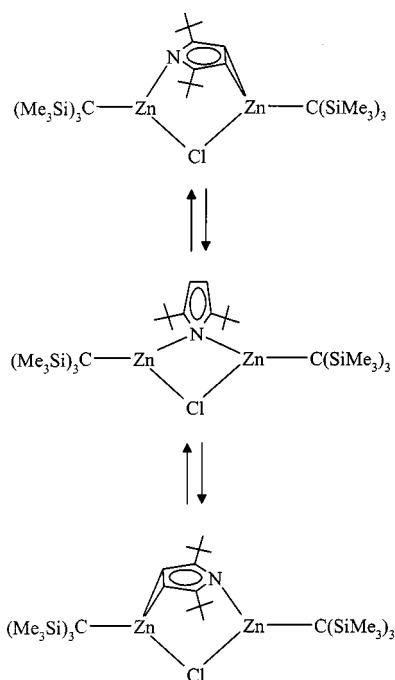
The mass spectrum of **4** shows the dissociation products **3** and [tris(trimethylsilyl)methyl]zinc 2,5-di(*tert*-butyl)pyrrolide if the sample is heated above the melting point. At 425 K, the mass peaks of these compounds are the signals of highest intensity, besides that at *m/z* 179 for H–Pyr\*. At 460 K, even fragments containing two zinc atoms and one chlorine atom are detected. Products of a dismutation reaction such as Zn[C(SiMe<sub>3</sub>)<sub>3</sub>]<sub>2</sub> or Cl–Zn–Pyr\* were not observed.

Due to the insensitivity of the NMR parameters to the hapticity of the Pyr\* ligand, the characterization of the In<sup>I</sup> derivative **5** is limited. In this case, the most significant results were obtained from Raman spectroscopy, although the In<sup>I</sup> derivative **5** decomposes during laser irradiation. For σ(M–N)- and σ(H–N)-bonded derivatives such as H–Pyr\*, Me<sub>2</sub>Ga–Pyr\*, and Me<sub>3</sub>Sn–Pyr\*, a characteristic polarized high-intensity band at approximately 1560 cm<sup>-1</sup> is observed. For the compounds In<sup>I</sup>[Pyr\*] (**5**) and Sn<sup>II</sup>[Pyr\*]<sub>2</sub>, this band is shifted to lower energies, appearing in the region 1500–1510 cm<sup>-1</sup>. On the other hand, other vibrations of the ring at lower frequencies are shifted to higher values [for example, 1124 (η<sup>1</sup>) → 1165 (η<sup>5</sup>) cm<sup>-1</sup>],

Table 1. NMR parameters of the 2,5-di(*tert*-butyl)pyrrolide ligand in HPyr\* (1), (thf)<sub>2</sub>LiPyr\* (2), [(Me<sub>3</sub>Si)<sub>3</sub>CZn]<sub>2</sub>(μ-Cl)(μ-Pyr\*) (4), and In<sup>I</sup>{Pyr}\* (5) compared with data for Sn{Pyr\*}<sub>2</sub><sup>[22]</sup>, Pb{Pyr\*}<sub>2</sub><sup>[3]</sup>, Me<sub>2</sub>Ga-Pyr\*<sup>[2]</sup> and Me<sub>3</sub>Sn-Pyr\*<sup>[21]</sup> (M{Pyr\*} symbolizes an η<sup>5</sup>-bonded, M-Pyr\* a σ<sub>N</sub>-bonded azacyclopentadienide moiety)

		1	2	4	5	Me <sub>2</sub> Ga-Pyr*	Sn <sup>II</sup> {Pyr*} <sub>2</sub>	Me <sub>3</sub> Sn-Pyr*	Pb <sup>II</sup> {Pyr*} <sub>2</sub>
<sup>1</sup> H NMR	Solvent	C <sub>6</sub> D <sub>6</sub>	[D <sub>8</sub> ]THF	C <sub>6</sub> D <sub>6</sub>	C <sub>6</sub> D <sub>6</sub>	C <sub>6</sub> D <sub>6</sub>	C <sub>6</sub> D <sub>6</sub>	C <sub>6</sub> D <sub>6</sub>	C <sub>6</sub> D
	CH <sub>3</sub> (M), (H <sup>1-N</sup> )	7.53	—	—	—	0.19	—	0.02	—
	CH <sub>3</sub> ( <i>t</i> Bu)	1.17	1.22	1.40	1.40	1.24	1.39	1.26	1.39
<sup>13</sup> C NMR	H <sup>3,4</sup>	5.93	5.59	6.22	5.96	6.23	5.47	4.86	5.51
	<sup>3</sup> J(H <sup>3,4</sup> , H <sup>1</sup> )	2.8	—	—	—	—	—	—	—
	C(M-Me)	—	—	—	—	0.95	—	-5.86	—
	<sup>1</sup> J(C,H)	—	—	—	—	124.3	—	129.8	—
	CH <sub>3</sub> ( <i>t</i> Bu)	30.67	32.77	34.63	32.44	32.9	32.01	30.57	32.69
	<sup>1</sup> J(C,H)	125.5	123.9	—	125.45	124.9	—	125.6	—
	C( <i>t</i> Bu)	31.24	33.47	[a]	32.73	32.5	33.78	34.59	33.31
	<sup>2</sup> J(C,H)	3.75	3.71	—	3.85	—	—	3.8	—
	C <sup>3,4</sup>	102.53	100.13	104.60	103.34	105.5	100.51	81.40	105.19
	<sup>1</sup> J(C <sup>3,4</sup> , H)	166.47	157.03	—	167.0	163.8	—	157.8	—
	<sup>2</sup> J(C <sup>3,4</sup> , H <sup>4,3</sup> )	7.0	5.49	—	6.2	—	—	—	—
	<sup>3</sup> J(C <sup>3,4</sup> , H <sup>1</sup> )	7.05	—	—	—	—	—	—	—
C <sup>2,5</sup>	139.46	146.72	148.57	153.55	145.3	162.30	173.33	161.71	

[a] Signal not detected.



which has to be interpreted in terms of a change of the π-system of the nitrogen heterocycle. Characteristic for the In<sup>I</sup> derivative **5** is the vibration In-Pyr\* at 170 cm<sup>-1</sup>, which is lower in energy by 60 cm<sup>-1</sup> compared to the In C<sub>5</sub> mode of the simple, unsubstituted indocene.<sup>[23]</sup>

Finally, it should be mentioned that theoretical investigations on a monomeric (hypothetical) 2,5-dimethylazaindocene In<sup>I</sup>(NC<sub>4</sub>H<sub>2</sub>Me<sub>2</sub>-2,5) predict a very short distance of 238 pm between the indium atom and the heterocycle.<sup>[24]</sup> Such a bond length is only comparable with the values determined for the permethylated indocenes In<sup>I</sup>(C<sub>5</sub>R<sub>5</sub>).<sup>[8][25]</sup>

## Conclusion

The diverse coordination modes adopted by the 2,5-di(*tert*-butyl)pyrrolide ligand have been illustrated by an η<sup>5</sup> coordination to an indium(I) atom as well as bridging between two zinc atoms. Whereas the properties of 2,5-di(*tert*-butyl)azaindocene (**5**) are approximately as one would expect by analogy with pentamethylindocene, the zinc derivative **4** shows a unique structure as well as surprisingly low reactivity. Not even treatment with excess lithium 2,5-di(*tert*-butyl)pyrrolide (**2**) leads to substitution of the chloride ligand by a pyrrolide anion. The reason for this lack of reactivity is the steric shielding of the central ClZn<sub>2</sub> moiety by two tris(trimethylsilyl)methyl and two *tert*-butyl groups. These demanding substituents also lead to an extension of the Zn-Cl, Zn-N and Zn-C distances.

This work has been generously supported by the *Deutsche Forschungsgemeinschaft* (DFG) and the *Fonds der Chemischen Industrie*.

## Experimental Section

**General:** All experiments and manipulations were carried out under argon purified by passage through BTS catalyst and P<sub>4</sub>O<sub>10</sub>. Reactions were performed in dried, thoroughly deoxygenated solvents using standard Schlenk techniques. The starting materials 2,5-di(*tert*-butyl)pyrrole (**1**),<sup>[6]</sup> indium(I) chloride,<sup>[5]</sup> and [tris(trimethylsilyl)methyl]lithium<sup>[26]</sup> were prepared by literature procedures. The extreme sensitivity of **5** has thwarted all attempts to prove its purity by elemental analysis.

**Bis(tetrahydrofuran-*O*)lithium 2,5-Di(*tert*-butyl)pyrrolide (**2**):** At -78°C, a solution of *n*-butyllithium (15% in hexane, 9.4 ml) was added dropwise to a solution of 2,5-di(*tert*-butyl)pyrrole (2.70 g, 15.1 mmol) in 50 ml of *n*-hexane. On warming to room temp., a colorless solid precipitated, which was collected. Washing with two portions of *n*-hexane and subsequent drying in vacuo gave lithium 2,5-di(*tert*-butyl)pyrrolide (2.65 g, 14.3 mmol, 95%, dec. at 197°C; lithium analysis for C<sub>12</sub>H<sub>20</sub>NLi: calcd. 3.75; found 3.7). Carrying

out this reaction in a solvent mixture of diethyl ether and tetrahydrofuran yielded colorless **2** after recrystallization from tetrahydrofuran at  $-30^{\circ}\text{C}$  (4.71 g, 14.3 mmol, 95%). Loss of THF at  $60^{\circ}\text{C}$ , m.p. of the residue  $348^{\circ}\text{C}$ . –  $^1\text{H}$  NMR ( $[\text{D}_8]\text{THF}$ ):  $\delta = 5.59$  [CH(Pyrr\*)], 1.22 [CMe<sub>3</sub>(Pyrr\*)]. –  $^{13}\text{C}$  NMR ( $[\text{D}_8]\text{THF}$ ):  $\delta = 146.72$  [C-2,5(Pyrr\*)], 100.13 [dd, C-3,4(Pyrr\*),  $^1J(\text{C}^{3,4}\text{H}) = 157.03$  Hz,  $^2J(\text{C}^{3,4}\text{H}^{4,3}) = 5.5$  Hz], 33.47 (CMe<sub>3</sub>), 32.77 (CMe<sub>3</sub>). –  $^7\text{Li}$  NMR ( $[\text{D}_8]\text{THF}$ ):  $\delta = 3.60$ . – IR (Nujol, CsBr):  $\nu = 1584\text{ cm}^{-1}$  w, 1560 w, 1487 m, 1459 m, 1450 sh, 1392 w, 1388 m, 1381 w, 1348 s, 1299 m, 1265 w, 1248 s, 1200 s, 1139 w, 1051 sh, 1040 vs, 983 m, 954 sh, 949 w, 910 m, 886 s, 848 w, 822 w, 764 w, 732 vs, 713 vs, 674 w, 622 w, 574 m, 519 s, 515 sh, 429 m, 405 w, 337 w. – MS (70 eV, sample temp. 293 K);  $m/z$  (%): 185 (4) [LiPyrr\*<sup>+</sup>], 179 (15) [HPyrr\*<sup>+</sup>], 164 (83) [HPyrr\*<sup>+</sup> – Me], 149 (18) [HPyrr\*<sup>+</sup> – 2Me], 115 (73), 72 (100) [thf<sup>+</sup>], 57 (21) [tBu<sup>+</sup>].

[Tris(trimethylsilyl)methyl]zinc Chloride (**3**): Tris(trimethylsilyl)methane (8.47 g, 36.4 mmol) was dissolved in a mixture of tetrahydrofuran (45 ml) and diethyl ether (8.5 ml). At  $0^{\circ}\text{C}$ , a solution of methyllithium in diethyl ether (27.7 ml, 1.6 M, 44.3 mmol) was added. After stirring for 8 h at room temp., the solution was heated under reflux for an additional 6 h to destroy the remaining methyllithium. At room temp., anhydrous ZnCl<sub>2</sub> (4.96 g) was added in small portions and the mixture was stirred for 8 h. All volatile materials were then removed in vacuo and the residue was redissolved in diethyl ether. The insoluble part of the residue (LiCl) was filtered off, and the ethereal solution was dried and concentrated. The solid material was sublimed at  $110^{\circ}\text{C}$  in vacuo to afford LiCl-free **3** (3.1 g, 9.3 mmol, 26%), m.p.  $211^{\circ}\text{C}$ . –  $^1\text{H}$  NMR ( $[\text{D}_8]\text{THF}$ ):  $\delta = 0.19$ . –  $^{13}\text{C}$  NMR ( $[\text{D}_8]\text{THF}$ ):  $\delta = 6.38$  [SiMe<sub>3</sub>,  $^1J(\text{SiC}) = 49.8$  Hz]. –  $^{29}\text{Si}$  NMR ( $[\text{D}_8]\text{THF}$ ):  $\delta = -2.75$ . – IR:  $\nu = 1462\text{ cm}^{-1}$  m, 1377 m, 1262 s, 1250 s, 861 vs, 842 vs, 784 w, 725 w, 673 m, 661 m, 630 w, 614 w. – MS (70 eV, sample temp. 360 K, source temp. 470 K);  $m/z$  (%): 315 (12.8) [M<sup>+</sup> – Me], 201 (100) [C(SiMe<sub>3</sub>)<sub>3</sub><sup>+</sup> – 2Me], 73 (27) [SiMe<sub>3</sub><sup>+</sup>]. – C<sub>10</sub>H<sub>27</sub>ClSi<sub>3</sub>Zn: calcd. C 36.13, H 8.19; found C 34.57, H 8.19.

Bis[tris(trimethylsilyl)methyl]zinc Chloride 2,5-Di(tert-butyl)pyrrolide (**4**): At  $0^{\circ}\text{C}$ , a solution of *n*-butyllithium (2.5 M in hexane) was added dropwise to a solution of **1** (0.65 g, 3.62 mmol) in 20 ml diethyl ether, so as to give a colorless suspension of **2**. Sublimed **3** (2.4 g, 7.2 mmol), dissolved in 20 ml of diethyl ether, was then slowly added to this suspension. Once a clear solution had been obtained, all volatile materials were removed in vacuo. The residue was redissolved in *n*-pentane and insoluble LiCl was filtered off. At  $-20^{\circ}\text{C}$ , colorless **4** co-crystallized with a stoichiometric amount of *n*-pentane (1.85 g, 2.1 mmol, 58%); dec. at  $75^{\circ}\text{C}$ . –  $^1\text{H}$  NMR (C<sub>6</sub>D<sub>6</sub>):  $\delta = 6.22$  [CH(Pyrr\*)], 1.40 [CMe<sub>3</sub>(Pyrr\*)], 0.32 [SiMe<sub>3</sub>]. –  $^{13}\text{C}$  NMR (C<sub>6</sub>D<sub>6</sub>):  $\delta = 148.57$  [C-2,5(Pyrr\*)], 104.60 [C-3,4(Pyrr\*)], 34.63 [CMe<sub>3</sub>], 7.13 [SiMe<sub>3</sub>]. – IR (Nujol, CsBr):  $\nu = 1364\text{ cm}^{-1}$  m, 1349 m, 1283 m, 1259 vs, 1248 vs, 1207 m, 1154 w, 1148 sh, 1077 w, 1047 m, 1021 m, 982 w, 860 vs, 850 sh, 797 s, 782 s, 749 m, 723 m, 673 s, 660 s, 621 m, 550 w, 529 w, 471 m, 442 w, 362 w. – MS (70 eV, sample temp. 425 K, source temp. 460 K);  $m/z$  (%): 611 (4.5) {[Me<sub>3</sub>Si<sub>3</sub>CZn]<sub>2</sub>Cl – CH<sub>2</sub><sup>+</sup>}, 473 (49.5) [(Me<sub>3</sub>Si)<sub>3</sub>CZnPyrr\*<sup>+</sup>], 458 (7.9) [(Me<sub>3</sub>Si)<sub>3</sub>CZnPyrr\*<sup>+</sup> – Me], 315 (54.9) [(Me<sub>3</sub>Si)<sub>3</sub>CZnCl<sup>+</sup> – Me], 295 (17.3) [(Me<sub>3</sub>Si)<sub>3</sub>CZn<sup>+</sup>], 216 (7.4) [(Me<sub>3</sub>Si)<sub>3</sub>C<sup>+</sup> – Me], 201 (30.5) [(Me<sub>3</sub>Si)<sub>3</sub>C<sup>+</sup> – 2Me], 179 (100) [HPyrr\*<sup>+</sup>]. – MS (70 eV, sample temp. 460 K, source temp. 460 K);  $m/z$  (%): 626 (1.3) [M<sup>+</sup> – 2SiMe<sub>3</sub> – 2MeH], 611 (15.3) {[Me<sub>3</sub>Si<sub>3</sub>CZn]<sub>2</sub>Cl – CH<sub>2</sub><sup>+</sup>}, 593 (100) [M<sup>+</sup> – Me – 2SiMe<sub>3</sub> – CH<sub>2</sub>], 315 (20.6) [(Me<sub>3</sub>Si)<sub>3</sub>CZnCl<sup>+</sup> – Me], 295 (98.1) [(Me<sub>3</sub>Si)<sub>3</sub>CZn<sup>+</sup>], 216 (8.7) [(Me<sub>3</sub>Si)<sub>3</sub>C<sup>+</sup> – Me], 201 (23.3) [(Me<sub>3</sub>Si)<sub>3</sub>C<sup>+</sup> – 2Me]. – C<sub>32</sub>H<sub>74</sub>ClNSi<sub>6</sub>Zn<sub>2</sub>: calcd. C 47.58, H 9.24, N 1.73; found C 47.65, H 9.23, N 1.44.

Indium(I) 2,5-Di(tert-butyl)pyrrolide (**5**): As described above, a suspension of LiPyrr\* was prepared from HPyrr\* (2.7 g, 15 mmol) and a stoichiometric amount of *n*BuLi in 50 ml of THF. At  $-110^{\circ}\text{C}$ , InCl powder (2.2 g, 14.6 mmol) was added. During warming to room temp., the orange color of InCl disappeared. Thereafter, the reaction mixture was stirred for an additional 10 h. The solution was then concentrated to a volume of approximately

Table 2. Crystallographic data of **1**, **1**·thf, **2**, and **4**, as well as details of the structure solution and refinement procedures

Compound	<b>1</b>	<b>1</b> ·thf	<b>2</b>	<b>4</b> ·0.67pentane
Formula	C <sub>12</sub> H <sub>21</sub> N	C <sub>16</sub> H <sub>25</sub> NO	C <sub>20</sub> H <sub>36</sub> LiNO <sub>2</sub>	C <sub>35.33</sub> H <sub>81.99</sub> ClNSi <sub>6</sub> Zn <sub>2</sub>
formula mass [g·mol <sup>-1</sup> ]	179.30	247.37	329.44	855.70
<i>T</i> [K]	163(2)	163(2)	193(2)	193(3)
Space group <sup>[28]</sup>	<i>P</i> 1 (No. 2)	<i>P</i> 2 <sub>1</sub> / <i>m</i> (No. 11)	<i>P</i> <i>n</i> <i>m</i> (No. 52)	<i>P</i> <i>n</i> <i>m</i> (No. 62)
<i>a</i> [pm]	944.28(5)	642.55(2)	1001.3(1)	1775.0(3)
<i>b</i> [pm]	1333.07(8)	1603.21(5)	1759.8(2)	1780.8(3)
<i>c</i> [pm]	1494.61(9)	802.46(2)	1177.7(2)	1575.6(2)
$\alpha$ [°]	83.516(1)	90	90	90
$\beta$ [°]	77.668(1)	98.194(2)	90	90
$\gamma$ [°]	80.239(1)	90	90	90
<i>V</i> [nm <sup>3</sup> ]	1.8056(2)	0.81821(4)	2.0752(5)	5.031(1)
<i>Z</i>	6	2	4	4
<i>d</i> <sub>calcd.</sub> [g·cm <sup>-3</sup> ]	0.989	1.004	1.054	1.130
$\mu$ [mm <sup>-1</sup> ]	0.057	0.062	0.065	1.172
<i>F</i> (000)	600	272	728	1848
Scan range [°]	1.4 < $\theta$ < 25	6.8 < $\theta$ < 26.4	2.7 < $\theta$ < 24.0	1.7 < $\theta$ < 26.0
Measured data	9291	4471	14180	5118
Unique data ( <i>R</i> <sub>int</sub> )	4903 (0.025)	1357	1596 (0.055)	5118
Parameters	382	97	128	406
<i>wR</i> <sup>2</sup> [ <sup>a</sup> ] (all data)	0.1437	0.1842	0.2760	0.1773
<i>R</i> <sup>1</sup> [ <sup>a</sup> ] (all data)	0.0806	0.0883	0.1015	0.0843
Data [ <i>I</i> > 2 $\sigma$ ( <i>I</i> )]	3551	1075	1362	3867
<i>R</i> <sub>1</sub> [ <sup>a</sup> ] [ <i>I</i> > 2 $\sigma$ ( <i>I</i> )]	0.0537	0.0703	0.0925	0.0599
Good <sup>[b]</sup> on <i>F</i> <sup>2</sup>	1.021	1.090	1.125	1.084
Residual density [e·Å <sup>-3</sup> ]	0.19/–0.28	0.38/–0.21	0.63/–0.26	1.10/–0.67

<sup>[a]</sup> Definition of the *R* values:  $R_1 = (\sum ||F_o| - |F_c||) / \sum |F_o|$ ;  $wR_2 = \{\sum [w(F_o^2 - F_c^2)] / \sum [w(F_o^2)]\}^{1/2}$  with  $w^{-1} = \sigma^2(F_o^2) + (aP)^2$ . – <sup>[b]</sup>  $s = \{\sum [w(F_o^2 - F_c^2)^2] / (N_o - N_p)\}^{1/2}$ .

20 ml and the precipitated LiCl was filtered off. All volatiles were then removed in vacuo. Subsequent sublimation at 80°C and  $5 \times 10^{-3}$  Torr yielded a fraction of InPyr\* still contaminated with traces of THF. A second sublimation gave colorless cuboids of InPyr\* (4.5 mmol, 31%). These crystals were found to be composed of very thin plates and proved unsuitable for an X-ray structure determination. For NMR data, see Table 1; for discussion of relevant IR/Raman data, see text. —  $C_{12}H_{20}NIn$  (293.12): calcd. In 39.17; found In 38.3 (complexometric titration), 38.9 (ICP).

*X-ray Crystallographic Studies:*<sup>[27]</sup> Suitable single crystals of **1**, **1-thf**, and **4** were covered with Nujol, mounted on a Siemens P4 diffractometer, and examined with graphite-monochromated  $MoK_{\alpha}$  radiation ( $\lambda = 71.073$  pm). For the collection of data sets for **1** and **1-thf**, the diffractometer was equipped with a Siemens SMART-CCD area detector. Due to its low melting point, compound **1-thf** was kept at temperatures below  $-30^{\circ}C$  during handling and mounting on the diffractometer. For the data collection of **2**, a STOE-IPDS diffractometer was used. Crystallographic parameters and details of the data collection are summarized in Table 2.

All structures were solved by direct methods with the software package SHELXTL-Plus<sup>[29]</sup> and refined with the program SHELXL-93.<sup>[30]</sup> Neutral atom scattering factors were taken from Cromer and Mann<sup>[31]</sup> and for the hydrogen atoms from Stewart et al.<sup>[32]</sup> The non-hydrogen atoms were refined anisotropically. The H atoms of **1** and **1-thf** were refined as a riding model with restriction of ideal geometry at the corresponding carbon atoms, whereas the nitrogen-bonded hydrogen atoms were refined isotropically. The H atoms of **2** were refined group by group to a common C–H bond length while maintaining ideal geometry at the corresponding C atoms, whereas the azacyclopentadienide-bonded hydrogen atoms were refined isotropically. The hydrogen atoms of **4** were refined isotropically, with the exception of those of the *tert*-butyl groups and of the *n*-pentane molecule, which were calculated in ideal positions with a C–H distance of 96 pm. The *n*-pentane molecules located between the molecules of **4** (Figure 6) were considered to have an occupancy factor of 0.67.

[1] R. King, M. Bisnette, *Inorg. Chem.* **1964**, *3*, 796.

[2] O. Schwarz, Ph.D. Thesis, University Stuttgart, in preparation.

[3] N. Kuhn, G. Henkel, S. Stubenrauch, *Angew. Chem.* **1992**, *104*, 766; *Angew. Chem. Int. Ed. Engl.* **1992**, *31*, 778.

[4] [4a] M. Porchia, F. Benetollo, N. Brianese, G. Rosetto, P. Zanello, G. Bombieri, *J. Organomet. Chem.* **1992**, *424*, 1. — [4b] J. Tödtmann, W. Schwarz, J. Weidlein, A. Haaland, *Z. Naturforsch.* **1993**, *48b*, 1437. — [4c] H.-D. Hausen, J. Tödtmann, J. Weidlein, *J. Organomet. Chem.* **1994**, *466*, C1. — [4d] H.-D. Hausen, J. Tödtmann, J. Weidlein, *Z. Naturforsch.* **1994**, *49b*, 430.

[5] F. Smith, R. Barrow, *J. Chem. Soc., Faraday Trans.* **1958**, *54*, 826.

[6] [6a] R. Ramasseul, A. Rassat, *Bull. Soc. Chim. Fr.* **1965**, 3136. — [6b] G. Gragnaire, R. Ramasseul, A. Rassat, *Bull. Soc. Chim. Fr.* **1969**, 415.

[7] M. Westerhausen, B. Rademacher, W. Schwarz, J. Weidlein, S. Henkel, *J. Organomet. Chem.* **1994**, *469*, 135 and references cited therein.

[8] O. T. Beachley Jr., R. Blom, M. R. Churchill, K. Faegri Jr., J. C. Fettinger, J. C. Pazik, L. Victoriano, *Organometallics* **1989**, *8*, 346.

[9] R. Hacker, E. Kaufmann, P. v. R. Schleyer, W. Mahdi, H. Diedrich, *Chem. Ber.* **1987**, *120*, 1533.

[10] [10a] M. A. Khan, D. G. Tuck, *Acta Crystallogr.* **1984**, *C40*, 60. — [10b] R. Gregorzik, H. Vahrenkamp, *Chem. Ber.* **1994**, *127*, 1857.

[11] M. Westerhausen, M. Wieneke, W. Schwarz, *J. Organomet. Chem.* **1996**, *522*, 137.

[12] *Struct. Rep.* **1960**, *25*, 283; *ibid.* **1961**, *26*, 319; *ibid.* **1978**, *43a*, 154.

[13] S. S. Al-Juaid, C. Eaborn, A. Habtemariam, P. B. Hitchcock, J. D. Smith, K. Tavakkoli, A. D. Webb, *J. Organomet. Chem.* **1993**, *462*, 45. See also the review: C. Eaborn, J. D. Smith, *Coord. Chem. Rev.* **1996**, *154*, 125.

[14] J. Behm, S. D. Lotz, W. A. Herrmann, *Z. Anorg. Allg. Chem.* **1993**, *619*, 849.

[15] T. Aoyagi, H. M. M. Shearer, K. Wade, G. Whitehead, *J. Organomet. Chem.* **1978**, *146*, C29.

[16] P. H. M. Budzelaar, J. Boersma, G. J. M. van der Kerk, A. L. Spek, A. J. M. Duisenberg, *J. Organomet. Chem.* **1985**, *281*, 123. See also the review: J. Boersma in *Comprehensive Organometallic Chemistry*, vol. 2 (Eds.: G. Wilkinson, F. G. A. Stone, E. W. Abel), Pergamon, Oxford, **1982**, chapter 16, p. 823.

[17] [17a] R. Blom, J. Boersma, P. H. M. Budzelaar, B. Fischer, A. Haaland, H. V. Volden, J. Weidlein, *Acta Chem. Scand.* **1986**, *A40*, 113. — [17b] B. Fischer, P. Wijkens, J. Boersma, G. van Koten, W. J. J. Smeets, A. L. Spek, P. H. M. Budzelaar, *J. Organomet. Chem.* **1989**, *376*, 223.

[18] [18a] A. Haaland, K. Hedberg, P. P. Power, *Inorg. Chem.* **1984**, *23*, 1972. — [18b] P. P. Power, K. Ruhlandt-Senge, S. C. Shoner, *Inorg. Chem.* **1991**, *30*, 5013. — [18c] W. S. Rees, D. M. Green, W. Hesse, *Polyhedron* **1992**, *11*, 1667.

[19] [19a] H. Grützmacher, M. Steiner, H. Pritzkow, L. Zsolnai, G. Huttner, A. Sebald, *Chem. Ber.* **1992**, *125*, 2199. — [19b] P. H. M. Budzelaar, J. Boersma, G. J. M. van der Kerk, A. L. Spek, *Organometallics* **1984**, *3*, 1187.

[20] [20a] W. A. Herrmann, I. Schweitzer, P. S. Skell, M. L. Ziegler, K. Weidenhammer, B. Nuber, *Chem. Ber.* **1979**, *112*, 2423. — [20b] K. Yünlü, F. Basolo, A. L. Rheingold, *J. Organomet. Chem.* **1987**, *330*, 221. — [20c] N. Kuhn, E.-M. Horn, R. Boese, D. Bläser, *Chem. Ber.* **1989**, *122*, 2275. — [20d] N. Kuhn, G. Henkel, J. Kreutzberg, *Angew. Chem.* **1990**, *102*, 1179; *Angew. Chem. Int. Ed. Engl.* **1990**, *29*, 1143.

[21] [21a] F. Glockling, N. S. Hosmane, V. B. Mahale, J. J. Swindall, L. Magos, T. J. King, *J. Chem. Res. (S)* **1977**, 116; *J. Chem. Res. (R)* **1977**, 1201. — [21b] C. Eaborn, N. Retta, J. D. Smith, *J. Organomet. Chem.* **1980**, *190*, 101. — [21c] M. Westerhausen, B. Rademacher, W. Poll, *J. Organomet. Chem.* **1991**, *421*, 175.

[22] N. Kuhn, G. Henkel, S. Stubenrauch, *J. Chem. Soc., Chem. Commun.* **1992**, 760.

[23] O. G. Garkusha, B. V. Lokshin, R. B. Materikova, L. M. Golubinskaya, V. I. Bregadze, A. P. Kurbakova, *J. Organomet. Chem.* **1988**, *342*, 282.

[24] A. Haaland, private communication, **1997**.

[25] H. Schumann, C. Janiak, F. Görlitz, J. Loebel, A. Diedrich, *J. Organomet. Chem.* **1989**, *363*, 243.

[26] [26a] A. H. Cowley, N. C. Norman, M. Pakulski, *Inorg. Synth.* **1990**, *27*, 235. — [26b] F. Schaller, W. Schwarz, H.-D. Hausen, K. W. Klinkhammer, J. Weidlein, *Z. Anorg. Allg. Chem.* **1997**, *623*, 1455.

[27] Crystallographic data (excluding structure factors) for the structures of **1**, **1-thf**, **2**, and **4** have been deposited with the Cambridge Crystallographic Data Centre as supplementary publication no. CCDC-101239. Copies of the data can be obtained on application to CCDC, 12 Union Road, Cambridge, CB2 1EZ, U.K. [Fax: (internat.) + 44(0)1223/336033; E-mail: deposit@ccdc.cam.ac.uk].

[28] T. Hahn (Ed.), *International Tables for Crystallography*, vol. A ("Space Group Symmetry"), 2nd ed., D. Reidel, Dordrecht, **1984**.

[29] SHELXTL Plus, PC version, Siemens Analytical X-ray Instruments, Inc., **1980**.

[30] G. M. Sheldrick, *SHELXL-93*, Universität Göttingen, **1993**.

[31] D. T. Cromer, J. B. Mann, *Acta Crystallogr.* **1968**, *24*, 321.

[32] R. F. Stewart, E. R. Davidson, W. T. Simpson, *J. Chem. Phys.* **1965**, *42*, 3175.

[98090]